Desalination and Water Treatment
www.deswater.com

doi: 10.1080/19443994.2016.1172988

57 (2016) 27469–27476
December

Taylor & Francis
Taylor & Francis Group

Modeling and simulation of a water distiller system operated by PV panels at real meteorological condition tests

Hanen Nafaa[a,*], Sina Ouriemi[b], Maissa Farhat[a], Sbita Lassaad[a]

[a]*Electrical and Automation Department, Research Unit of Photovoltaic, Wind and Geothermal systems, National Engineering School of Gabes, University of Gabes, Street of Mednine, 6029 Gabes, Tunisia, emails: hanen_nafaa@yahoo.fr (H. Naffa), maissa.farhat@gmail.com (M. Farhat), lassaad.sbita@enig.rnu.tn (S. Lassaad)*

[b]*Chemical Engineering Processes Department, Higher Institute of Technological Studies of Gabes, Street of Mednine, 6011 Gabes, Tunisia, email: soueriemi@gmail.com*

Received 5 February 2016; Accepted 27 March 2016

ABSTRACT

Three-quarters of the surface of our planet is covered by water. Nevertheless, these inexhaustible reservoirs like oceans are not suitable for drinking because it is salt water. This work deals with water desalination as a solution to the water scarcity problem. It presents a new process of solar distillation that naturally produces distilled water. The essential features of this process are summarized by the production of heat via electric resistor. In this work, the photovoltaic source is feeding the resistive load. The simulation work was elaborated under the real meteorological conditions of Gabes, a city in the south of Tunisia. In order to optimize the photovoltaic system efficiency, a maximum power point tracker that controls a DC–DC boost converter is used. The system was implemented and then tested on a sunny day under variable resistance combination. The simulation results show that increasing the number of panels increases the quantity of distilled water; on the other hand, the parallel association of resistances improves the time needed for the distillation of water.

Keywords: Photovoltaic energy; Solar generator; Boiling in tubes; Desalination

1. Introduction

One of the basic requirements for all living things is the availability of pure drinking water [1]. Nowadays, the global water demand is continuously increasing due to population growth and economic development [2]. Water demand will grow in the future. Desalination of seawater and brackish water can be used to face the increasing demand for freshwater supplies [3]. However, desalination is a very energy-consuming process, often using energy supply from fossil fuel sources, which cause pollution and present logistical supply problems in remote and island communities. They are therefore not sustainable.

There are two broad categories of desalination technologies. Membrane desalination uses pressure or electricity to separate freshwater from seawater or brackish water using a membrane, while thermal desalination uses heat to vaporize freshwater [4]. There has been a lot of published literature on thermal desalination, such as multi-effect distillation (MED). This technique generally consumes much energy. It

*Corresponding author.

would be profitable if free or low-cost heat energy were available. Hybrid processes such as MEAD could also be used [5]. In this paper, we designed a new system that uses photovoltaic energy, as it is low-cost, unlimited, and renewable.

This paper focuses primarily on water desalination through the use of renewable energy. Renewable technologies that are suited to desalination include solar thermal, solar photovoltaic, wind, and geothermal energy [6]. Solar technologies based on solar heat concentration, notably concentrating solar power, produce a large amount of heat that is suited to thermal desalination. Photovoltaic and wind electricity are often combined with membrane desalination units (reverse osmosis and electrodialysis). As electricity, storage is still a challenge, combining power generation and water desalination can also be a cost-effective option for electricity storage when generation exceeds demand. In particular, Photovoltaic (PV) technology can be connected directly to membrane desalination technology, which is based on electricity as the input energy. Many small PV-based desalination systems have been demonstrated throughout the world [7], especially in remote areas and islands. This paper also covers other photovoltaic technology systems. Among the several options to connect a seawater desalination system with a photovoltaic power plant, the present photovoltaic model is used as the heat source. This system is the least energy consuming. Other solar systems use energy to implement the pump and produce heat at the same time, which consumes more energy.

The new process of photovoltaic distillation naturally produces distilled water. The essential features of this process consist in producing heat by the electric resistance, which is connected to the photovoltaic panel. This process is produced on a small dimension. It presents an environmentally friendly desalination solution that addresses the major issues of the water–energy–environment nexus [8].

2. Description of the system

The boiler apparatus comprises an electric heating copper wire submerged in water; it is horizontally mounted in a cylindrical vertical glass chamber. There is a water distiller that comprises a vaporization chamber and a tube condenser coiling.

The details of the chamber are as follows: an upper vertical tube having an open bottom and a closed top communication with the condenser, the receptacle of the portable water distiller is automatically kept full with water up to a predetermined level, and the lower portion of the tube has access to the heating element. Under Fig. 1, there is an illustration of the heating element, which is an electric resistance that keeps the water at boiling temperature under atmospheric pressure. “ab” is a metal test wire of *l* length; its ends are welded to “aA” and “bB”, respectively. These silver- or nickel-plated copper wires are d in diameter. A, B are connected to copper wires of larger diameter which carry the electric current to supply the necessary heat to “ab”. The electric power going through the wires is provided by photovoltaic panels. This phenomenon is termed “pool boiling”.

The first experimental work on the pool boiling owes to Nukiyama [9,10]. For this experiment, an electrically heated copper wire is immersed in a bath of distilled water maintained at 100°C. The flux density is obtained by measurements of the current and the voltage across the wire and the average temperature of the wall is inferred from the variation of the resistance of the wire with respect to temperature as shown in the Fig. 1.

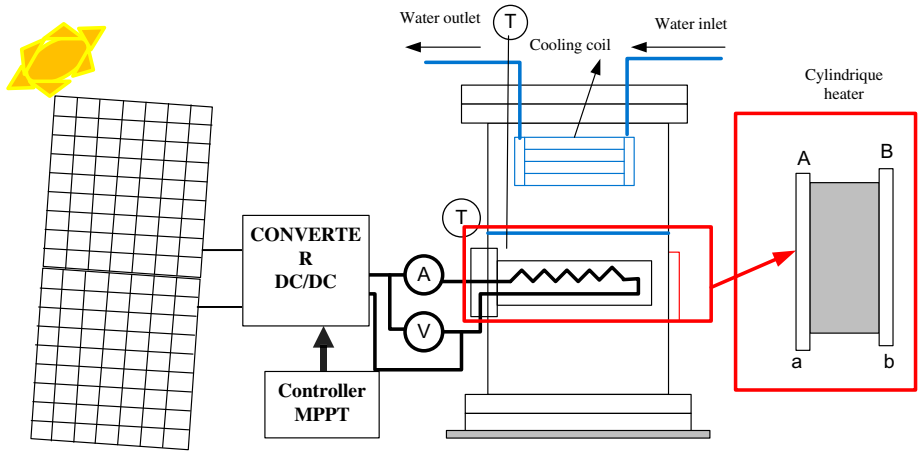

Fig. 1. The glass vessel for distilled water.

3. Mathematical modeling of the system and simulation

3.1. Solar energy analysis for photovoltaic generation

The design of a photovoltaic system depends on the density of the solar flux. However, the variation of the density of the solar flux is random. Therefore, a solar flux model is necessary. In this work, the solar flux model has been created and then compared to the real meteorological data of Gabes city.

After much work on solar models, namely the ASHRAE, DELORME, and EUFRAT models [11], the EUFRAT model has been chosen for the calculation of global solar flux for the city of Gabes as a result of its efficiency. The EUFRAT model was developed to provide the parameters required for any day of the year.

The EUFRAT model is based on the synthesis of various works, especially those of Brichambant, Kasten, and hay. In calculating, the energy illumination model uses the atmospheric disturbance through linked disorder factor β. This factor is estimated locally by the formula [12]:

$$\beta = 1.6 + 16 \cdot \beta_a + 0.5 \cdot \ln(P) \quad (1)$$

where P is the water vapor pressure and β_a is the coefficient angstrom according to the operating conditions.

The values that can take β_a are summarized in Table 1.

The determination of the density of the overall solar flux requires determination of some astronomical quantities necessary for calculation.
The model requires the calculation [13]:

Declination:

$$\delta = 23.45 \sin\left(360\left(\frac{248 + q}{365}\right)\right) \quad (2)$$

True solar time:

$$\mathrm{TSV} = \mathrm{TU} + \mathrm{CC} \quad (3)$$

Table 1
Values of the coefficient β_a [12]

Type clear sky	β_a
Deep blue	0.02
Pure blue	0.05
Light blue	0.1
Whitish	0.
Milky blue	0.2

Hour angle:

$$w = 15 \cdot (12 - \mathrm{TSV}) \quad (4)$$

The height of the sun:

$$\sin h = \sin \varphi \cdot \sin \delta + \cos \varphi \cdot \cos \delta \cdot \cos \omega \quad (5)$$

The determination of the density of the overall solar flux (Gh) requires the quantities calculated by the previous equations, using the Eq. (1) and those required to calculate:
Correction coefficient distance earth-sun:

$$\alpha = 1 + 0.034 \cos\left(\frac{360q}{365}\right) \quad (6)$$

Air mass crossing:

$$\mathrm{AM} = \frac{(1 - 0.1\,A1)}{\sin h} \quad (7)$$

The density of the direct irradiation at normal incidence [11]:

$$I_n = I_0\,\alpha \exp\left(\frac{-AM\beta}{0.9\,AM + 9.4}\right) \quad (8)$$

The density of horizontal global irradiation:

$$G_h = \alpha(1270 - 56\beta)(\sin h)^{\frac{\beta+36}{33}} \quad (9)$$

To validate the model, we chose typical days. We chose for the study 20 July 2011. Fig. 2 shows comparisons between experimental and calculated data of irradiation.

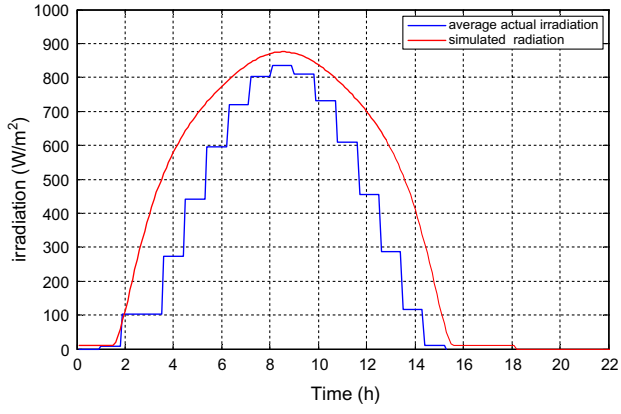

Fig. 2. Solar irradiation intensity of the solar panel in function of time.

3.2. Photovoltaic generation system

An ideal solar cell is modeled by a current source in parallel with a diode. However, no solar cell is ideal, and therefore shunt and series resistances are added to the model as shown in the Fig. 3.

The PV array model [14] that is widely used is the one-diode model. It is composed of subsystems with a specific number of cells in series and/or parallel. The relationship between current and voltage for one cell is given by:

$$I = N_p I_{ph} - I_d - I_{sh} \tag{10}$$

The diode current is given by the Shockley's diode equation [15]:

$$I_d = I_{sat}\left(\exp\left(\frac{V + IR_s}{TKn_s}q\right) - 1\right) \tag{11}$$

The reverse saturation current I_{sat}, is dependent upon temperature, and is described in this equation:

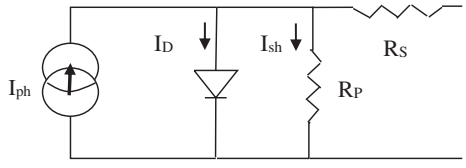

Fig. 3. The solar PV panel model.

$$I_{sat} = I_{RS}\left(\frac{T}{T_{REF}}\right)^3 \exp\left[\frac{qE_g\left(\frac{1}{T_{REF}} - \frac{1}{T}\right)}{KA}\right] \tag{12}$$

with

$$I_{RS} = \frac{I_{SC}}{\exp\left(\frac{qV_{OC}}{n_S K T_C A}\right) - 1} \tag{13}$$

The photocurrent of the module I_{ph}, can be calculated as:

$$I_{ph} = \text{lamda}(I_{SC} + K_1(T - T_{REF})) \tag{14}$$

with

$$\text{Lamda} = \frac{G}{G_S} \tag{15}$$

The Shunt current is given by:

$$I_{sh} = \frac{(V + IR_S)}{R_p} \tag{16}$$

With the aforementioned equations, a model simulate the PV panel in MATLAB/SIMULINK was created. Fig. 4 illustrates the I-V and P-V characteristics of the PV panels.

The simulation was at a solar temperature 25°C and irradiation 1,000, 500, and 300 W/m^2, when the PV panels were connected to resistive loads R. The

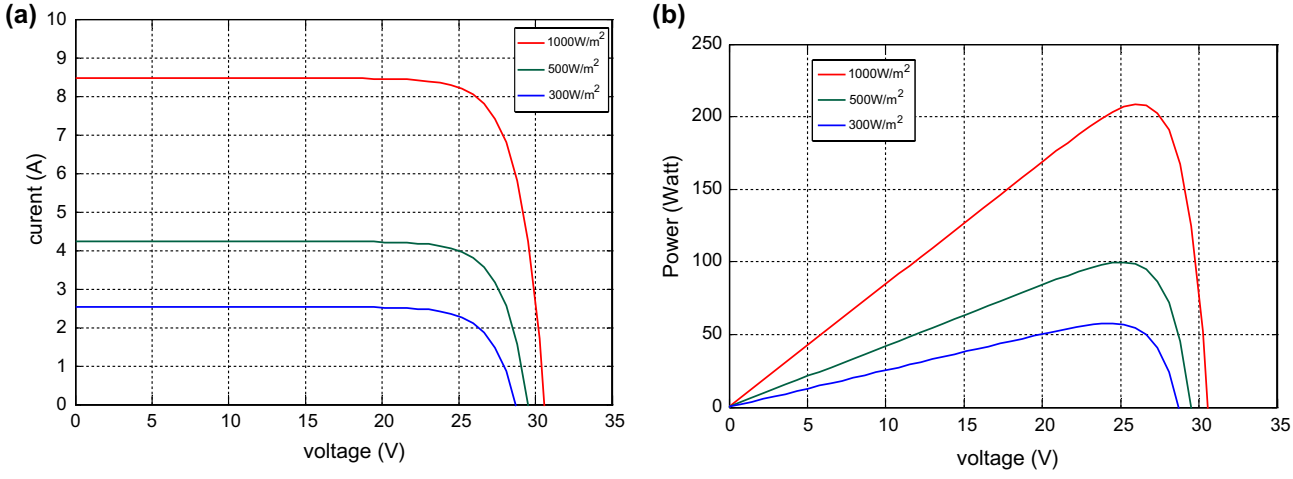

Fig. 4. (a) V-I and (b) P-V characteristic for PV panel.

Table 2
Parameters of PV-TD195HA6 solar module

Parameters PV Cell	Value	Unit
Short circuit current ISC	8.48	A
Short circuit voltage VOC	30.6	V
Maximum power voltage	25.4	V
Maximum power current	7.69	A
Ideal factor (A)	1.2	–
Boltzmann's constant (K)	1.38 e-23	J/K
Number of cells	50 cell as in a series	–
Electron charge (q)	1.6 e-19	Cb

parameters chosen for modeling correspond to the MITSUBISHI electric photovoltaic module PV-TD 195HA6 [16] as listed in Table 2.

3.3. DC–DC converter

The function of the generator is highly dependent on the characteristics of the load with which it is connected. In addition, for different values of R, optimal adaptation takes place for one operating point (Rop) named maximum Power point tracker (MPPT). As a result, the generator works most often at its maximum point, the solution commonly used is to introduce a DC–DC converter that acts as a source-charge adapter. Thus, the generator delivers maximum power.

One of the major problems of PV systems is that the output voltage of PV panels is highly dependent on solar irradiance and ambient temperature; hence, loads cannot be directly connected to the output of PV panels. These systems usually consist of a PV generator and a load. However, direct interfacing between PV generator and load introduces significant mismatch problems as the light intensity varies. The mismatch can be overcome by introducing a matching DC–DC converter that continuously seeks PWM of PV generator. This converter can be controlled by a PWM controller (P&O) [17]. The principle of this controller is to provoke perturbation by acting (decreasing or increasing) on the PWM duty cycle command and observing the output PV power reaction.

The boost converter is DC–DC [18], which increases its input voltage and resistance following the equation in (17):

$$V_{out} = \frac{1}{1-D} V_{in}$$
$$R_{in} = (1-D)^2 R_{ch} \quad (17)$$

where V_{out} is the output voltage of the boost converter, V_{in} the input voltage, R_{in} the input resistor, R_{ch} the load resistor, and D *is* the duty cycle [19].

The boost converter is shown in Fig. 5.

3.4. Steam flow estimated

Saturated water is boiled on a horizontal wire, which functions as an electric resistance heater and as resistance thermometer. The wire, heated by Joule effect, is placed in an electrical circuit which passes a current intensity I. If U is the potential difference across the wire, the electrical power P dissipated in the wire is connected to the heat flow density q by the relation:

$$P = U \times I = q \times S \times l = RI^2 \quad (18)$$

where d and l, respectively, correspond to the diameter and length of the wire. q is the heat transmitted from the metal surface per area unit per time unit to the water.
with

$$S = \Pi \left(\frac{d}{2}\right)^2 \quad (19)$$

The resistance is given by:

$$R = R_0(1 + \alpha \Delta T) \quad (20)$$

where R_0 is resistance of initial value, α is the temperature coefficient of the resistance, and ΔT is the temperature variation.
with

$$R_0 = \frac{\rho l}{S} \quad (21)$$

where ρ stands for the resistivity of copper.

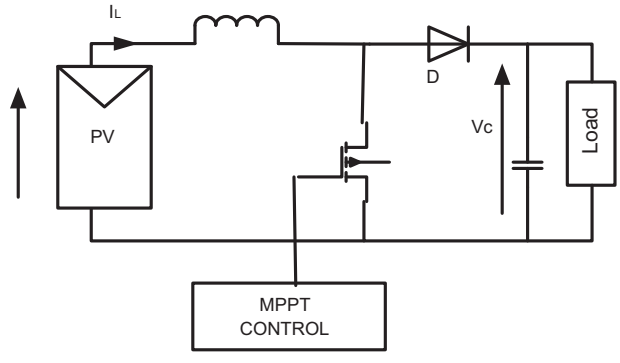

Fig. 5. Schema of the boost converter.

In general, in boiling vapor takes place either on the exterior surface of submerged tubes or on the interior surface. Pool boiling refers to vaporization that takes place at a solid surface submerged in a quiescent liquid. When the temperature, T_s, of the solid surface exceeds the saturation temperature, T_{sat}, of the liquid, vapor bubbles form at a nucleation sites on the surface, grow, and subsequently detach from the surface.

The temperature of the wire (T_s) is assumed to be consistent. It is determined through knowledge of its electrical resistance [20].

One of the first and most useful correlations for nucleate boiling was that of Rohsenow in 1952 [20]:

$$\frac{C_{pL(T_S-T_{sat})}}{\Delta H_V} = C_{sf}\left[\frac{q}{\eta_L \Delta H_v}\sqrt{\frac{\sigma_L}{g(\rho_L-\rho_V)}}\right]^{\frac{1}{3}}\left(\frac{\eta_L C_{PL}}{\lambda_L}\right)^{n} \quad (22)$$

where all properties for liquid are at T_{sat}. The constant C_{sf} is an empirical coefficient depending mainly on the surface condition and the nature of the liquid. The parameter of this equation is mentioned in Table 3.

The exponent n depends on the type of fluid. For the water, we take n to be 1.

Finally, we have:

$$(T_s - T_{sat})^3 = \frac{q}{\mu_L \times \Delta H_v}\left(\frac{\sigma_L}{g(\rho_L-\rho_v)}\right)^{\frac{1}{2}}\left[\frac{C_{sf}\Delta H_V P_{rl}}{C_{pL}}\right]^3 \quad (23)$$

The surface tension of water in contact with its vapor is given by:

$$\sigma_{water} = 235.8\left(1-\frac{T_{sat}}{T_c}\right)^{1256}\left[1-0.625\left(1-\frac{T_{sat}}{T_C}\right)\right]\left(\frac{mN}{m}\right) \quad (24)$$

where T_{sat} and T_c are expressed in K. The evaporation rate (the water quantity evaporated per unit time) flow of water evaporated is given by:

$$\dot{m} = \frac{P}{(\Delta H_V + C_P \Delta T)} \quad (25)$$

With the aforementioned equations, a model simulating the boiling apparatus in MATLAB/SIMULINK was created. The values of all the parameters are given in the above; with $n = 1$, P is panel power. At operating pressure: $p = 1$ atm = 1.013 bar.

The simulation of the system for a day was performed as well. In this simulation, variable solar intensity was used. The values of those parameters were obtained for a typical summer day in June in GABES from EUFRAT model. Fig. 6 shows the

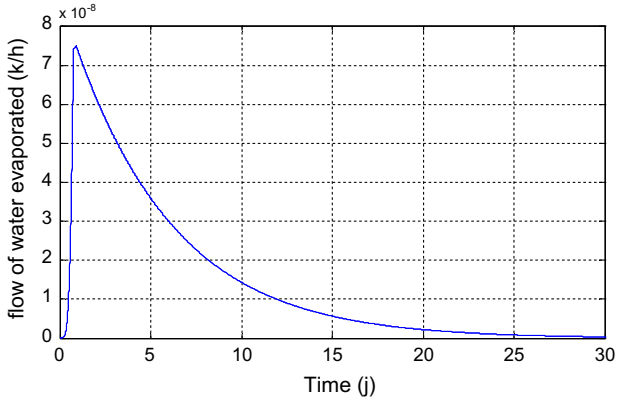

Fig. 6. Daily distillate production for one PV.

Table 3
Thermophysical parameters of pure water at atmospheric pressure

Symbol	Property	Value	Unit
C_{sf}	Surface roughness factor	0.013	–
C_{PL}	Specific heat at constant pressure of water	4.21	kJ/(kg K)
G	Gravitational acceleration	9.81	m/s^2
T_c	Thermodynamic critical temperature	647.096	K
T_{sat}	Saturation temperature of water	100	℃
ΔH_v	Latent heat of vaporization	2,260	kJ/kg
ρ_L	Density of saturated water	958	kg/m^3
ρ_V	Density of saturated vapor	0.6	kg/m^3
λ_L	Thermal conductivity	0.68	W/(m K)
μ_L	Dynamic viscosity	2.82×10^{-4}	Pa s
$P_{rL} = \frac{C_{PL}\cdot\mu_L}{\lambda_L}$	Prandtl number of water	1.746	–

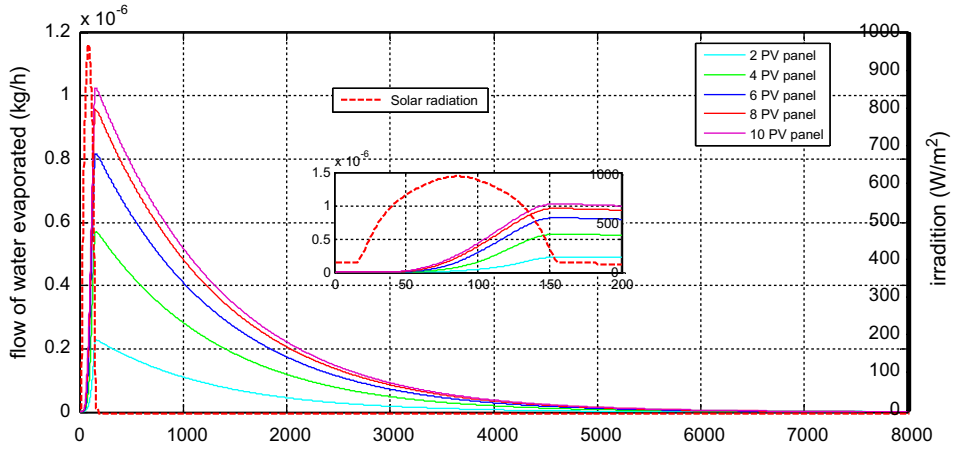

Fig. 7. Daily distillate production for different numbers of PV panel associations.

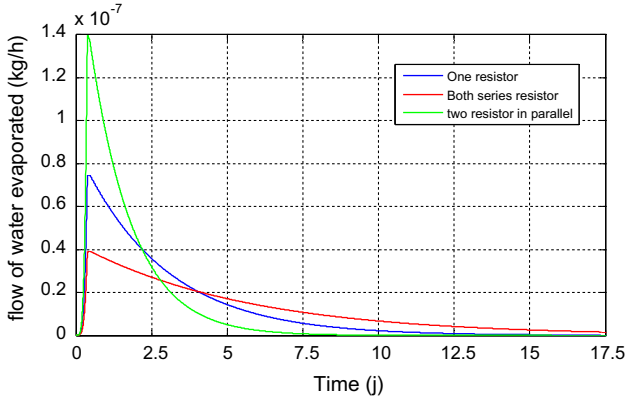

Fig. 8. Daily distillate production for different resistor associations.

variations of the cumulative distillate, during the day. In this simulation, the water flow rate was estimated at 2.7016×10^{-4} kg/m^2 after a month for one irradiation day.

Fig. 7 shows the cumulative distillate production for one day of operation. The graph shows that for a given thermal storage volume there is an optimum combination of PV panel number. A series of 10 PV panels produces a rate of evaporated water that is equivalent to 0.0013 kg/m^2 d of the accumulated distilled water. However, for two PV panels we have just 2.7016 e-004 kg/m^2.

The simulation results show that increasing the number of panels increases the quantity of distilled water; on the other hand, the association of resistance in parallel improves the time needed for distillation of water. Fig. 8 shows the effect of resistance association system.

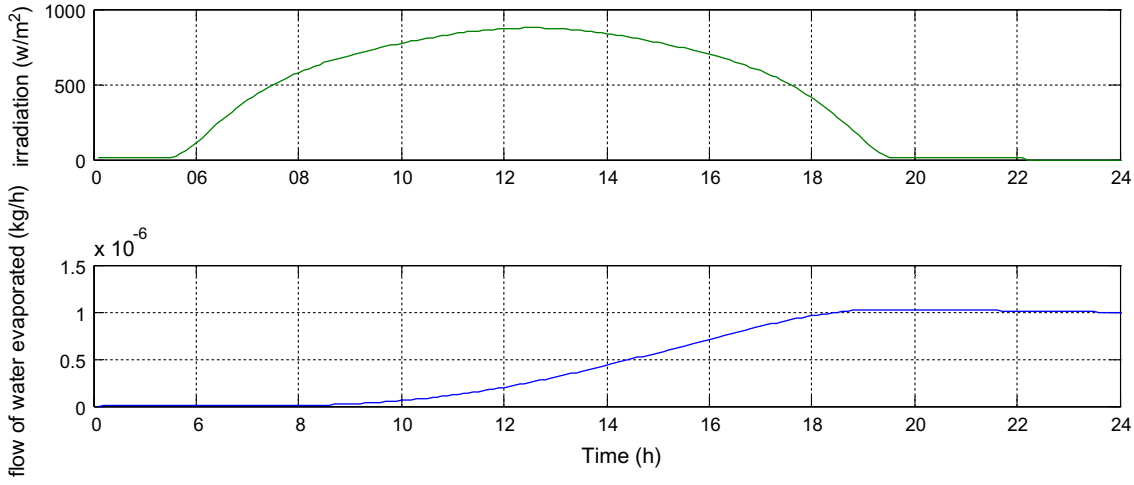

Fig. 9. Thermal performance of the system.

Fig. 9 shows that the water takes time to heat up. When it reaches the boiling temperature, it begins to produce distillate. Then, the change in production remains almost constant for a period of time when irradiation decreases, production decreases (especially at night).

4. Conclusion

The present research aims at studying the simulation of a desalination system coupled with PV panels. In order to study the contribution of the solar energy effect, a model describing the water distiller system is developed. This model comprises different connections of panels and resistances. The results obtained show that the desalination system performance is remarkably influenced by the number of PV panels connected. The coupling of the parallel resistor allows the improvement of the time distillation that can be reached during the day. Yet, production could be enhanced with the use of hybrid distillation, which ensures high elevations of temperature.

References

[1] J. Huckle, A. Martin, Environments in a Changing World, Routledge, New York, NY, 2014.
[2] M. Flörke, E. Kynast, I. Bärlund, S. Eisner, Domestic and industrial water uses of the past 60 years as a mirror of socio-economic development: A global simulation study, Global Environ. Change 23 (2013) 144–156.
[3] N. Ghaffour, T.M. Missimer, G.L. Amy, Technical review and evaluation of the economics of water desalination: Current and future challenges for better water supply sustainability, Desalination 309 (2013) 197–207.
[4] D. Emadzadeh, W.J. Lau, T. Matsuura, M. Rahbari-Sisakht, A.F. Ismail, A novel thin film composite forward osmosis membrane prepared from PSf–TiO_2 nanocomposite substrate for water desalination, Chem. Eng. J. 237 (2014) 70–80.
[5] M.W. Shahzad, K. Thu, Y.-D. Kim, K.C. Ng, An experimental investigation on MEDAD hybrid desalination cycle, Appl. Energy 148 (2015) 273–281.
[6] N. Ghaffour, S. Lattemann, T. Missimer, K.C. Ng, S. Sinha, G. Amy, Renewable energy-driven innovative energy-efficient desalination technologies, Appl. Energy 136 (2014) 1155–1165.
[7] V.G. Gude, N. Nirmalakhandan, S. Deng, Renewable and sustainable approaches for desalination, Renewable and Sustainable Energy Rev. 14 (2010) 2641–2654.
[8] B.B. Saha, I.I. El-Sharkawy, M.W. Shahzad, K. Thu, L. Ang, K.C. Ng, Fundamental and application aspects of adsorption cooling and desalination, Appl. Therm. Eng. 97 (2016) 68–76, doi: 10.1016/j.applthermaleng09.(2015).113.
[9] S. Nukiyama, The maximum and minimum values of the heat transmitted from metal to boiling water under atmospheric pressure, Intl. J Heat Mass Transfer 27 (1984) 959–970.
[10] I.C. Chu, H.C. No, C.H. Song, D.J. Euh, Observation of critical heat flux mechanism in horizontal pool boiling of saturated water, Nucl. Eng. Des. 279 (2014) 189–199.
[11] R. Mechlouch, A. El Jery, A.B. Brahim, Choix d'un modèle d'ensoleillement et détermination des inclinaisons optimales des capteurs héliothermiques pour la ville de gabes en Tunisie, Rev. Energies Renouvelables 6 (2003) 1–15.
[12] B. Bourges, Climatic Data Hand Book for Europe, Kluwer Dordrecht, France, 1992, pp. 2–8.
[13] A.J. Duffie, W.A. Beckman, Solar Engineering of Thermal Processes, Wiley, Canada, 1980.
[14] M. Farhat, F. Aymen, S. Lassaad, Influence of photovoltaic DC bus voltage on the high speed PMSM drive, IEEE International Conferences IECON'2012 (2012) 4489–4494.
[15] M. Farhat, O. Barambones, L. Sbita, Real-time efficiency boosting for PV systems using MPPT based on sliding mode, Energy Procedia 75 (2015) 361–366.
[16] Available from: <http://www.aprosios.com>.
[17] P. Surma, Comparison of methods of photovoltaic panels MPPT (P & O, IC, Fuzzy Logic) in Matlab Simulink, przegląd elektrotechnicznyl, ISSN 90 (2014) 33–2097.
[18] G. Farivar, B. Asaei, A new approach for solar module temperature estimation using the simple diode model, IEEE Trans. Energy Convers. 26 (2011) 1118–1126.
[19] M.H. Rachid, Power Electronics Circuits Devices and Applications, third ed., Prentice-Hall of India, New Delhi, 2014, pp. 220–227.
[20] J. Battaglia, A. Kusiak, J.-R. Puiggali, Introduction aux transferts thermique, Dunod, Paris, 2014, pp. 142–146.